E6-2003-31

CATALOGUE OF RADIONUCLIDE LOW-ENERGY ELECTRON SPECTRA (LEES)

JOINT COMMUNICATION

DLNP (JINR), Dubna, Russia
CSNSM (IN2P3-CNRS), Orsay, France
BNM-LNHB (LIST/DIMRI), CEA, Saclay, France

Tz. Vylov, V. M. Gorozhankin, A. Kovalik, E. A. Yakushev, M. Mahmoud,
A. F. Novgorodov, N. A. Lebedev, D. Filosofov
Joint Institute for Nuclear Research, Dubna, Russia

Ch. Briancon, R. Walen
CSNSM-CNRS, Orsay, France

N. Coursol
BNM-LNHB (LIST/DIMRI), CEA, Saclay, France

A. Minkova, P. Petev
University of Sofia, Bulgaria

O. Dragoun, V. Brabec
INR, Rez, Czech Republic

A. Inoyatov
IAP, National University, Tashkent, Republic of Uzbekistan

© Joint Institute for Nuclear
Research, 2003

Introduction

Three different electron emission processes take part in the decay of radioactive nuclei: nuclear β-decay, nuclear-atomic interaction (internal conversion of γ-radiation), and atomic shell relaxation (Auger and Coster-Kronig transitions). Electron spectra from radioactive decay contain information on both the nature of the process responsible for electron emission and nuclear and/or atomic properties. Accordingly, precise data on electron spectra have a crucial importance for a variety of topical fundamental and applied problems.

Only one edition [1] of a catalogue of conversion electron spectra exists so far. It presents spectra of over 60 neutron-deficient radionuclides with Z = 56–71, which have been measured using semicircular focusing beta spectrographs.

The present catalogue contents systematically recorded spectra so as energies, and emission intensities of conversion and Auger electrons accompanying radioactive decay of radionuclides with Z = 24–95, measured with the electrostatic spectrometer ESA-50.

1. Precision spectrometry of low-energy electrons from radioactive decay

1.1 Spectrometers

Extensive studies of electron emission spectra from radioactive decay started in the second half of the 1950s, when the first magnetic electron spectrometers were built in many nuclear physics laboratories (see refs. [2, 3]). These spectrometers were either with homogeneous flat magnetic field, either iron-free or iron-core spectrometers with current coils. Despite of their good spectrometric characteristics and sometimes unique design, nearly all of them had a low-energy limitation ($E_e \geq 30$ keV). This limitation was mainly due to the technically difficult problem of producing weak magnetic fields with the desired parameters to achieve very high instrumental resolution ($\Delta p/p < 0.1\%$).

In the mid-1960s the development of photoelectron and Auger-electron spectroscopy as methods for chemical analysis of surfaces (ESCA) [4, 5, 6] led to a renewal of instrumental development in the laboratories active in this field, in particular the electrostatic electron energy analysers. Owing to their small size, the relative simplicity of getting electrostatic fields of a few kV with the desired configuration, electrostatic spectrometers turned out to be more appropriate for analysis of electrons in the energy range from 1 eV to 3 keV. This encouraged well-known companies to launch mass production of electron spectrometers of various types and designs using sources of exciting radiation (usually ultraviolet or X-rays).

These spectrometers had an important drawback from the nuclear physics point of view: any attempt to extend the analysed energy range beyond 3 keV resulted in deterioration of their focusing properties due to relativistic effects. The precision electron spectrometry in the energy range from 3 keV to 30 keV now focuses the research attention in connection with some currently important problems of nuclear and atomic physics such as spectroscopy of strongly converted low-energy nuclear transitions, study of radiationless relaxations of atomic shells in radioactive decay and their application, recent problems related to estimation of the electron antineutrino rest mass from the tritium beta-spectrum, *etc.*

1.2 Electron sources

The high instrumental resolution of the spectrometer is a necessary but not sufficient requirement to achieve an appropriate accuracy level in the low-energy electron spectrometry ($E_e < 30$ keV) with radioactive sources. *Quality* of radioactive electron source is also of crucial importance.

A high sensitivity of the instrumental line shape to the source quality is caused by the large specific electron energy loss on its way through a source of finite thickness and by the backscattering from a source backing. The estimated mean free path for inelastic collision of electrons with energy of several keV in solid ranges from one to several $\mu g/cm^2$ (nm), which is equivalent to several monoatomic layers for most elements.

The aforesaid defines the main requirements to the initial radioactive preparations and the source characteristics. The radioactive preparation procedure has to insure:

- the highest possible radiochemical purity;
- the highest possible chemical purity;
- a high specific activity.

The electron sources must have:

- homogeneous distribution of activity over the backing surface;
- minimum thickness of the active layer;
- stability of the source for oxidation, evaporation, diffusion, *etc*;
- conducting backings of small *Z*.

The widely used methods for source preparation in electron spectroscopy are electrolytic precipitation, ion implantation, and vacuum evaporation [7]. A new method based on monomolecular Langmuir–Blodgett layers was recently proposed [8]. However, none of these methods is universal and therefore the choice depends on the particular problem and experimental conditions.

2. Spectrometry of low-energy electrons from radioactive decay with the ESA-50 electrostatic spectrometer

2.1 Electrostatic spectrometer ESA-50

The electrostatic spectrometer ESA-50 [9] is constructed to measure electron spectra in the energy range $E_e = 0.1–50$ keV. It is the first instrument for research in nuclear physics which combine two types of analysers, *integral* (spherical decelerator) and *differential* (double cylindrical mirror) ones. The relativistic effects arising in spectrometry of fast electrons and typical for one analyser spectrometers are eliminated in this combination.

The spectrometer and related systems are schematically shown in Fig. 1. The decelerator is a sphere at ground potential and has a concentric conic slot as input slit of the cylindrical mirror analyser. The radioactive source is placed in the sphere center where positive decelerating voltage U is applied. Only electrons of energy high enough to pass the retardation potential of the decelerator can enter in the cylindrical mirror field.

Decelerated electrons are focused by a double cylindrical mirror analyser. The analyzing voltage u is applied to its outer cylinder. The spectrum is scanned by varying the decelerating voltage U at constant analysing voltage u. In this working mode the energy of electrons recorded by the detector and the absolute instrument resolution ΔE remain constant over the whole

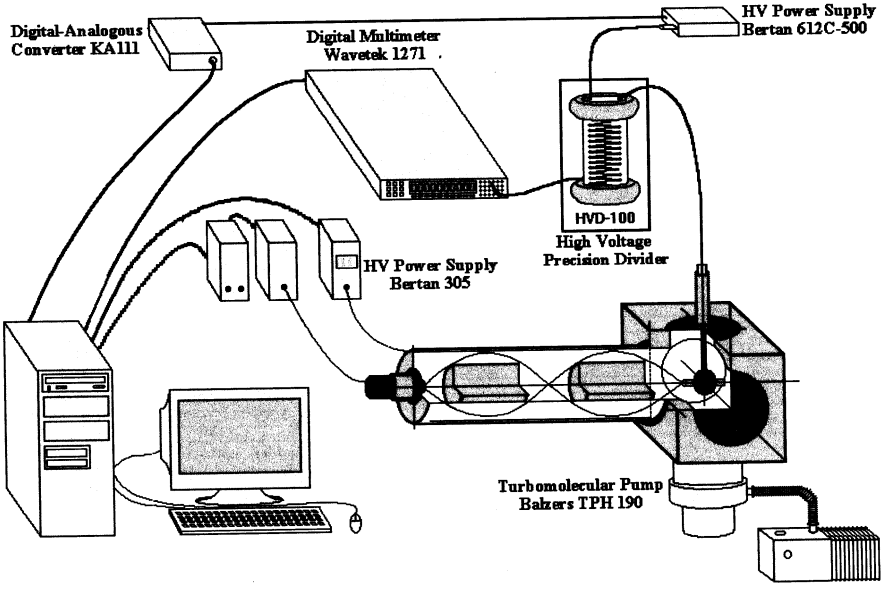

Fig. 1. Principal scheme of the ESA-50 spectrometer and its control system.

measured energy region. The energy of electrons entering the cylindrical mirror analyser is $E_a = E_e + qU$, where $q = -1$ is the electron charge, while for transmission through cylindrical mirror analyser $E_a = buq$, where b is an instrument constant.

The geometrical parameters and the calculated instrument constant are [10]: $r_1 = 50$ mm; $r_2 = 105$ mm; $r_s = 42$ mm; $2L = 615$ mm; $b = 1.83$, where r_1 and r_2 are the radii of the inner and outer mirror cylinders respectively, r_s is the spherical decelerator radius, $2L$ is the source-detector distance.

The instrumental resolution ΔE can be adjusted according to the experimental necessities by simply varying the analysing voltage u across the cylindrical mirror. Higher resolution is attained when $|u|$ has small values. However, in this case the total transmission of the spectrometer also decreases.

The data acquisition and control system, fully automated by using a PC (Fig. 1), allows the decelerating voltage U to be varied in steps of 0.1 V (minimum) and provides its stabilization at the level of 10^{-5}.

The electrons are recorded by the Optotechnik KBL-15RS channel electron multiplier, which have a 15 mm in diameter input window. The spectrometer is shielded against external magnetic fields by a magnetic screen system consisting of three long cylinders of μ-metal placed inside the vacuum chamber and covering the entire space between the source and the detector. Several additional short cylinders of the same material protect the space around both ends of the long cylinders. The residual magnetic field in the spectrometer is less than 1 mG.

The vacuum system of the spectrometer based on the Balzers TPH-190 turbomolecular pump, provides oil-free vacuum of $\sim 7 \times 10^{-7}$ mBa.

The design of the spectrometer allows one optimize the analysing electrostatic field distribution and reduction of the negative effect of scattered electrons on the apparatus spectra.

The characteristics of the spectrometer have been investigated by using ^{169}Yb and ^{57}Co sources (Fig. 2). The measured energy resolution limit (at u= –50 V) ΔE = 4.8 eV for E_e=7.3 keV includes the natural width of the conversion line and some continuous energy losses. Estimation

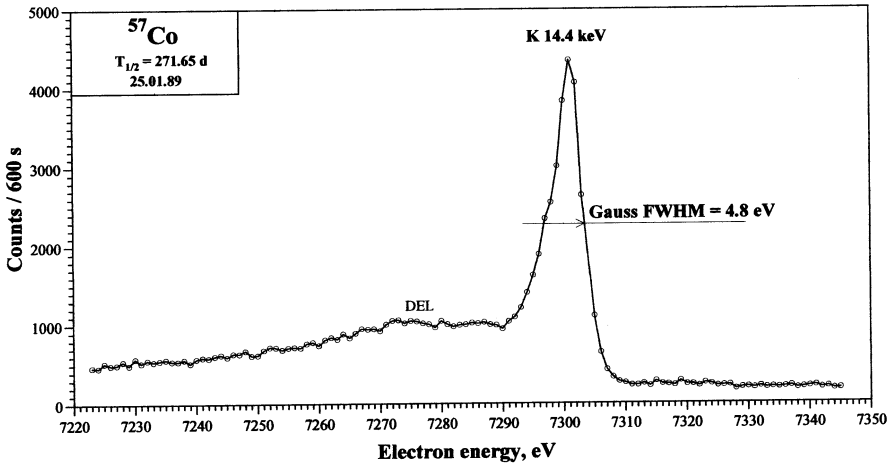

Fig. 2. The K internal conversion electrons of the 14.4 keV nuclear transition in ^{57}Fe measured with the ESA-50 spectrometer (DEL – discrete energy losses).

of the absolute spectrometer efficiency at this resolution in the same energy range yielded the value of 0.1% of 4π.

2.2 Production of radionuclides

The initial activity has usually been produced (see Table 1) in the following reactions:

- (n,γ) induced by irradiation of appropriate targets with thermal neutrons from the reactors of Research Institute for Atomic Reactors in Dimitrovgrad (n = $5x10^{15}$ $s^{-1}cm^{-2}$) and IBR-2 in FLNP, JINR (n = 2×10^{12} $s^{-1}cm^{-2}$);
- (α,xn) and (d, xn) induced by irradiation of targets at the U-120 cyclotron (FLNR, JINR);
- deep spallation induced by irradiation of targets with proton beam of E_p = 660 MeV from the Phasotron facility (DLNP, JINR).

Commercial isotopes delivered by the company IZOTOP were also used.

A chemical treatment of the irradiated targets consisted in their dissolving and subsequent chromatographic separation of the desired radionuclides. Sometimes isotope separation of the element fraction has been carried out with an electromagnetic mass separator. In this case the collector with the accumulated activity was dissolved and the radioisotope chemically separated from the collector material. The activity was thoroughly purified and concentrated at each step of its radiochemical separation.

2.3 Preparation of radioactive electron sources

The electron sources have been prepared by the vacuum evaporation method [11] or by the modified Langmuir–Blodgett method [12].

The vacuum evaporation method consisted of two procedures. The first procedure was deposition by electrolysis of the purified and concentrated radioactive material onto an evaporator of high melting point material. The second procedure included low-temperature (500–600°C) degassing to remove all the highly volatile impurities and then high-temperature evaporation and deposition of the radioactive material onto source backing. A tantalum foil, purified by annealing, and with a recess for electrolysis, was usually used as evaporator . The evaporation and deposition onto the backing was done at the commercial facility VUP-4. The backing was rotated (~2000 rpm) to insure azimuthal uniformity of deposition.

The method of monomolecular Langmuir–Blodgett layers (MMLBL) is based on the property of molecules of organic surfactants (such as aliphatic acids, ketones, alcohols) to have a certain orientation in the water-air interface: the hydrophilic part of the molecule faces the water while its hydrophobic part faces the air. Chemisorption of surfactant cations by stabilized oriented molecules results in formation of a practically monoatomic layer on the surfactant surface and provides the basis of this method for preparation of monolayer sources.

The order of steps in source preparation by the MMLBL method is as follows. The first step is the formation of the MMLBL and its transfer to a metal backing. Then, 30–100 μl of the concentrated radionuclide solution is dropped onto the MMLBL. The chemisorption time depends on the specific activity of the initial preparation and the prescribed final activity of the source. When the chemisorption is completed the remained solution is removed from the MMLBL surface and the surface itself is thoroughly washed by bidistilled water.

The physical and chemical conditions for preparation of radioactive monolayer sources, the methods of their transfer to a solid backing and their properties are experimentally studied in refs.[13–15]. The results of these experiments have shown that the conditions for source preparation by this method have to be selected individually for each nuclide or a group of nuclides with similar chemical properties.

In general, the source quality using the MMLBL method is comparable with the quality of sources prepared by the vacuum evaporation method and it remains stable for a long time irrespective of storage conditions (vacuum, atmosphere).

2.4. Energy calibration of the spectrometer

The energy scale of an electron spectrometer is determined by measuring of spectra with conversion lines of well known energies at the assumption that the relationship between the electron energy E_e and the spectrometer voltage is linear.

The energy calibration accuracy depends on the following conditions:

- using of conversion lines of nuclear transitions which energy is known to a high accuracy;
- correct accounting for the effect of the radionuclide chemical state on the electron binding energies [4, 5];
- precision of the spectrometer control system;
- high energy resolution of the spectrometer;
- using of conversion lines with small natural widths.

The radionuclides that might be used for calibration of an electron spectrometers in the low-energy region are very limited. The main selection criteria for calibration radionuclides are the presence of well enough studied low-energy nuclear transitions, reasonable half-lives, stability of the physical and chemical properties of the source , and availability. The conversion lines of the

nuclear transitions 14.4130(3) keV [16] (^{57}Co – ^{57}Fe decay), 8.4101(2) keV [17], and 20.7438(1) keV [18] (^{169}Yb – ^{169}Tm decay) were used for energy calibration. The vacuum deposition method were used for preparation of these sources.

The relationship between the electron energy E_e and the deceleration voltage for the ESA-50 spectrometer is given by the equation $E_e = q(cu - U)$, where q = -1, b = 1.83. Experimental verification [19] of this relationship in the energy range 6–20 keV did not reveal deviations larger than 2 eV.

It should be however noted, that the line position has some small shift depending on the backing material [20]. As one goes from aluminium to carbon the electron energy increases by 1.4 eV and in the case of platinum the shift is 2 eV. This effect was ignored in the calibration measurements because backing material other than aluminium was very rarely used. Nevertheless this effect should be taken into account in interpretation of spectra measured with sources on backings of other materials.

2.5. Spectrometer transmission

The electron spectra were measured in the working mode of scanning the decelerating voltage U at constant analysing voltage u across the cylindrical mirror. The instrumental electron line width and the electron energy as recorded by the detector are constant in the whole scanning range of U (or E_e). This scanning mode eliminates the necessity of corrections for the detector efficiency.

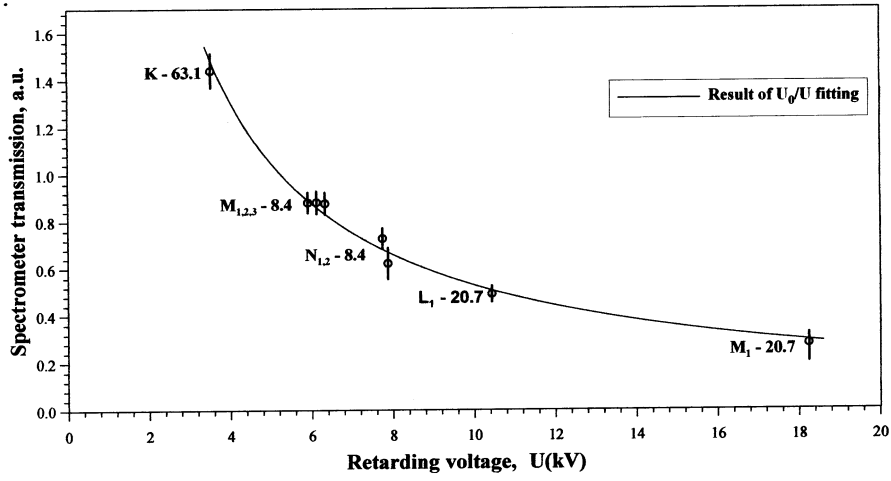

Fig. 3. A transmission dependence of the ESA-50 spectrometer (u=100 V).

However, in this working mode increase of decelerating voltage leads to a substantial decrease of the spherical decelerator transmission. Precise calculations of the relationship between the transmission and the deceleration voltage is a rather difficult task. Thus, this relationship had to be experimentally found by using the intensities of conversion lines of the nuclear transitions 8.4, 20.7, and 63.1 keV in the ^{169}Yb–^{169}Tm decay [19]. The relationship between the spectrometer transmission and deceleration voltage U at the analysing voltage u=100 V (Fig. 3) is quite well approximated by the function $1/U$ in the energy range of interest.

2.6. Spectra processing

The recorded spectrum $S(E_e)$ of electrons in the energy range $E_1 - E_2$ is a convolution of the energy distribution function $f(E'_e)$ of electrons leaving the source with the spectrometer response function $F(E_e,E'_e)$, $S(E_e) = \int_{E_2}^{E_1} f(E'_e) \times F(E_e,E'_e)dE'$. Since the true form of these functions is not precisely known, various model approximations are used to describe the experimental spectrum. Obviously, the accuracy and reliability of the spectrum processing depends on how close to the true line shape the approximations are.

In principle, the spectrometer response function $F(E_e,E'_e)$ can be simulated by the Monte Carlo method. Obviously, this technique requires comprehensive information on the spectrometer parameters, the magnitude and configuration of the analysing and scattered fields in the real spectrometer. This information is usually not available because the real spectrometer characteristics differ from the calculated ones. The theoretical response function in dispersion beta-spectrometers is quite well approximated by a Guassian function.

The most difficult problem to deal with is the energy distribution $f(E'_e)$ of electrons leaving the source. In the ideal case the energy distribution $N_e(E_e,E_{e0})$ of conversion and Auger electrons emitted in radioactive decay is described in view of the physical nature of these processes, by a Lorentz function, $N_e(E_e,E_{e0}) \sim [(E_e - E_{e0})^2 - (\Gamma/2)^2]^{-1}$, where Γ is the Lorentzian width equal in first approximation to the natural widths of the atomic levels participating in electron emission. In the real case the Lorentzian-like shape is deformed, predominantly in its low-energy part, because of numerous intra- and extra-atomic processes [5] accompanying the emission of electrons.

The electron energy loss, unavoidable in real conditions gives the dominating contribution to the Lorentzian deformation in experiments with the solid radioactive sources, mostly used in electron spectroscopy. A variety of analytical and semi-empirical expressions [21, 22] as well as standard computer codes for Monte Carlo calculations [23, 24] can be used for evaluation, with varying accuracy, of the inelastic electron energy losses in matter over a wide energy range. However, the formal approach of resolving the problem does not work with real sources because it is necessary to take into account the source composition, thickness, and homogeneity, the effect of its surface layer, the electron backscattering function, possible diffusion of radioactive atoms into the source backing, *etc*. Obviously, it is impossible to provide full information on the source, including all the intra-atomic processes. This information has to be obtained by independent studies. Nevertheless the contribution of each mentioned above process is included, to a greater or lesser extent, in the energy distribution $f(E'_e)$.

Thus, the theoretical description of conversion and Auger electron spectra with allowance for all mechanisms for instrumental line shape formation is an extremely difficult problem at present.

The most realistic approaches are those using a combination or superposition of one or several analytical expressions or an instrumental line shape represented in tabulated form. To describe the instrumental line measured with the spectrometer ESA-50 both approaches have been used and the corresponding computer codes ERIKA [25] and BRUNDIBAR [26] were developed.

In the computer code ERIKA the shape of the single electron line is expressed by a many-parameter Gaussian-like function of the form [27]

$$L_j(i,a_1,\ldots a_8) = a_8^{(j)}\{\exp(-a_4((i-a_7^{(j)})^2) + [a_1\exp(i-a_7^{(j)})) + a_5\exp(a_6(i-a_7^{(j)}))]\times$$

$\times[1-\exp(-a3a4(i-a_7^{(j)})^2)]\}$ for $i \le a_7^{(j)}$

and

$$L_j(i,a_1,..a_8) = a_8^{(j)} \exp((-a_4(i-a_7)^2) \qquad \text{for } i > a_7^{(j)},$$

where $a_1 \ldots a_6$ are the line shape parameters identical for all lines in the spectrum under processing; $a_7^{(j)}$ and $a_8^{(j)}$ are the position and the height of the jth line respectively. The χ^2 function is minimized by the simplex method [28].

In the computer code BRUNDIBAR the so-called experimental Instrumental Line Shape (ILS) is used. It is represented in tabulated form and includes the spectrometer response function and the electron energy loss in the measured source and influences of intra- and extra-atomic processes. The experimental ILS is chosen from measured single conversion lines close in energy to the lines to be processed. If no such line is available the ILS has to be constructed from several lines in the measured spectrum. The spectrum is calculated as a convolution of the ILS with Lorentzian of width Γ, equal to the difference between the natural widths of the line to be described, and the line taken as the ILS

$$S(E_e) = \sum_{j=1}^{n} a_j \int_{-\infty}^{+\infty} \frac{(\Gamma_j/2^2)}{(E_e' - E_{e,0}^{(j)})^2 + (\Gamma_j/2^2)} ILS(E_e, E_e') dE_e',$$

where n is the number of lines in the spectrum; $E_e^{(j)}$, a_j, and Γ_i are the position, amplitude and width of the jth line, respectively. The parameters to be fitted are $E_e^{(j)}$ ($j = 1 \ldots n$), a_j, and the background.

3. Presentation of results

The studied radionuclides are presented in Table 1 in the order of increasing atomic number Z and/or mass number A. The table also gives an additional information on the decay mode, half-life, and method for the initial activity production.

Each spectrum in the catalogue is presented in this table by its code number, the measured energy range, instrumental resolution, focusing voltage in the cylindrical analyser, and the step of scanning by the decelerating voltage U.

The code name assigned is a sequence of four numerals denoting, first to last,

- the mass number;
- the atomic number of the parent radionuclide;
- the type of radiation (1 for α, 2 for β, 3 for γ, as in [29]);
- the code number.

Table 2 presents references where more detailed information on experimental conditions and results can be found.

CD Catalogue purchase information is available in the Publishing Department of JINR:
Joint Institute for Nuclear Research, Publishing Department, Joliot-Curie Str., 6
141980 Dubna, Moscow region, RUSSIA

E-mail: publish@pds.jinr.ru

Table 1. Total list of electron spectra included in the LEES Catalogue.

Source nucleus	Decay mode	Daughter nucleus	$T_{1/2}$	Production means	Spectrum name	Energy region, keV	Instrumental resolution, eV	u volts	Step eV	Spectrum Code	Presented spectrum
1	2	3	4	5	6	7	8	9	10	11	12
$^{51}Cr_{24}$	EC	$^{51}V_{23}$	27.701(6) d	$^{50}Cr(n,\gamma)$	KLL Auger	3.9 - 4.45	7	100	2	51-24-2-1	+
					KLM Auger	4.45 - 5.0	7	100	2	51-24-2-2	
$^{54}Mn_{25}$	EC	$^{54}Cr_{24}$	312.20(4) d	$^{53}Cr(d,n)$	KLL Auger	4.25 - 4.85	7	100	2	54-25-2-1	+
					KLM Auger	5.0 - 5.45	7	100	2	54-25-2-2	
$^{55}Fe_{26}$	EC	$^{55}Mn_{25}$	2.685(10) y	$^{54}Fe(n,\gamma)$	KLL Auger	4.7 - 5.2	3.5	50	2	55-26-2-1	+
					KLM Auger	5.5 - 5.8	3.5	50	2	55-26-2-2	
					KMM Auger	6.17 - 6.5	7	100	1	55-26-2-3	
$^{57}Co_{27}$	EC	$^{57}Fe_{26}$	271.65(13) d	$^{60}Ni(p,\alpha)$	Review	0.3 - 14.6	10	150	6	57-27-2-1	
					Review (log scale)	0.3 - 14.6	10	150	6	57-27-2-2	+
					LMX Auger	0.35 - 0.92	3.5	50	2	57-27-2-3	
					KLL, KLM, KMM Auger + K14.4 ICEs *	5.0 - 7.45	7	100	2	57-27-2-4	
					K14.4 ICEs	7.26 - 7.33	2.7	25	0.2	57-27-2-5	
					L_{1-3}14.4 ICEs	13.15 - 13.78	7	100	1	57-27-2-6	
					M_{1-3}14.4 ICEs	14.15 - 14.46	7	100	1	57-27-2-7	
$^{63}Ni_{28}$	β^-	$^{63}Cu_{29}$	100.1(20) y	$^{62}Ni(n,\gamma)$	Review (log scale)	0.4 - 25.2	7	100	50	63-28-2-1	+
$^{65}Zn_{30}$	EC, β^+	$^{65}Cu_{29}$	244.1(2) d	$^{63}Cu(\alpha,pn)$	Review	0.7 - 9.2	21	300	5	65-29-2-1	
					Review (log scale)	0.7 - 9.2	21	300	5	65-29-2-2	+
					LMX Auger	0.52 - 1.4	14	200	2	65-29-2-3	
					KLL Auger	6.25 -7.15	14	200	2	65-29-2-4	
$^{67}Ga_{31}$	EC	$^{67}Zn_{30}$	78.26(7) h	$^{65}Cu(\alpha,2n)$	Review	0.56 - 10.4	14	200	4	67-31-2-1	
					Review (log scale)	0.56 - 10.4	14	200	4	67-31-2-2	+
					LMX Auger	0.22 -1.46	3.5	50	1	67-31-2-3	
					KLL Auger	6.7 - 7.73	7	100	2	67-31-2-4	
					KLM Auger	7.93 - 8.73	7	100	2	67-31-2-5	
					KMM Auger	9.12 - 9.74	14	200	2	67-31-2-6	

1	2	3	4	5	6	7	8	9	10	11	12
$^{73}As_{33}$	EC	$^{73}Ge_{32}$	80.30(6) d	$^{72}Ge(d,n)$	Review	0.3 -15	7	100	10	73-33-2-1	
					Review (log scale)	0.3 -15	7	100	10	73-33-2-2	+
					LMX Auger, K13.26 ICEs	0.32 - 2.4	7	100	2	73-33-2-3	
					KLL Auger	7.8 - 8.6	7	100	2	73-33-2-4	
					L_{1-3}13.26, M_{1-3}13.26 ICEs	7.2 - 13.3	7	100	2	73-33-2-5	
					L_{1-3}13.26, M_{1-3}13.26 ICEs (log scale)	7.2 - 13.3	7	100	2	73-33-2-6	
$^{83}Rb_{37}$	EC	$^{83}Kr_{36}$	86.2(1) d	Zr(p;xp,yn)	Review	0.4 - 18.1	14	200	5	83-37-2-1	
					Review (log scale)	0.4 - 18.1	14	200	5	83-37-2-2	+
					LMX Auger	0.89 - 1.59	7	100	2	83-37-2-3	
					KLL Auger	10.3 - 11.0	7	100	2	83-37-2-4	
					KLM Auger	11.9 - 12.7	7	100	2	83-37-2-5	
					KMM Auger	13.5 - 14.3	7	100	2	83-37-2-6	
					L_{1-3}9.4 ICEs	7.3 - 7.8	7	100	2	83-37-2-7	
					M_{1-3}9.4 ICEs	8.8 - 9.3	7	100	2	83-37-2-8	
$^{103}Pd_{46}$	EC	$^{103}Rh_{45}$	16.961(16) d	$^{102}Pd(n,\gamma)$	Review	0.31 - 25.4	10	150	10	103-46-2-1	
					Review (log scale)	0.31 - 25.4	10	150	10	103-46-2-2	+
					KLL Auger	16.2 - 17.15	3.5	50	2	103-46-2-3	
$^{111}In_{49}$	EC	$^{111}Cd_{48}$	2.83(1) d	$^{109}Ag(\alpha,2n)$	Review	0.5 - 27	14	200	10	111-49-2-1	
					Review (log scale)	0.5 - 27	14	200	10	111-49-2-2	+
					MNX Auger	0.18 - 4.2	2.5	30	10	111-49-2-3	
					MNX Auger (log scale)	0.18 - 4.2	2.5	30	10	111-49-2-4	
					LMX Auger	1.1 - 4.1	3.5	50	1	111-49-2-5	
					KLL Auger	17.6 - 19.7	14	200	2	111-49-2-6	
					KLM Auger	21.2 - 23.2	7	100	4	111-49-2-7	
					KMM Auger	24.7 - 26.8	21	300	2	111-49-2-8	
					KNN Auger	26.4 - 26.87	35	500	3	111-49-2-9	

1	2	3	4	5	6	7	8	9	10	11	12
$^{131}I_{53}$	β^-	$^{131}Xe_{54}$	8.040(1) d	Fission	Review	0.8 - 28.8	28	400	10	131-53-2-1	
					Review (log scale)	0.8 - 28.8	28	400	10	131-53-2-2	+
					MNX Auger	0.1 - 0.73	3.5	50	2	131-53-2-3	
					LMX Auger	2.5 - 4.5	14	200	2	131-53-2-4	
$^{131}Cs_{55}$	EC	$^{131}Xe_{54}$	9.688(4) d	$^{130}Ba(n,\gamma)^{131}Ba(EC)$	Review	0.72 - 34.0	21	300	10	131-55-2-1	
					Review (log scale)	0.72 - 34.0	21	300	10	131-55-2-2	+
					MNX Auger	0.11 - 1.1	3.5	50	1	131-55-2-3	
					LMX Auger	2.1 - 5.25	3.5	50	1	131-55-2-4	
					KLL Auger	23.15 - 25.15	7	100	2	131-55-2-5	
					KLM Auger	27.2 - 30.2	14	200	5	131-55-2-6	
$^{140}Nd_{60}$	EC	$^{140}Pr_{59}$	3.37(2) d	Gd(p;xp,yn)	Review	1.2 - 36.0	35	500	20	140-60-2-1	
	EC	$^{140}Ce_{58}$	3.39(1) m		Review (log scale)	1.2 - 36.0	35	500	20	140-60-2-2	+
					MNX Auger	0.32 - 3.2	7	100	3	140-60-2-3	
					MNX Auger (log scale)	0.2 - 4.0	-	10-2000	40	140-60-2-4	
					KLL Auger	26.5 - 30.3	35	500	10	140-60-2-5	
$^{145}Sm_{62}$	EC	$^{145}Pm_{61}$	340(3) d	Er(p;xp,yn)	$L_3M_{1-5}M_{1-5}$ Auger	2.75 - 4.65	14	200	2	145-62-2-1	
	EC	$^{145}Nd_{60}$	17.7(4) m		K61.25 ICEs	15.79 - 16.15	3.5	50	2	145-62-2-2	
					KLL Auger	29.6 - 32 6	35	500	5	145-62-2-3	+
$^{146}Eu_{63}$	EC, β^+	$^{146}Sm_{62}$	4.59(3) d	Er(p;xp,yn)	LMX Auger	2.9 - 6.6	14	200	2	146-63-2-1	+
$^{155}Eu_{63}$	β^-	$^{155}Gd_{64}$	4.96(1) y	$^{154}Sm(n,\gamma)^{155}Sm(\beta^-)$	Review	0.31 - 25.7	10	150	10	155-63-2-1	
					Review (log scale)	0.31 - 25.7	10	150	10	155-63-2-2	+
					LMX Auger	2.8 - 7.4	7	100	5	155-63-2-3	
					M_{1-3}18.8 ICEs	16.35 - 17.4	7	100	5	155-63-2-4	
					L_{1-3}21.0 ICEs	12.2 - 13.6	7	100	5	155-63-2-5	
$^{155}Tb_{65}$	EC	$^{155}Gd_{54}$	5.32(6) d	Er(p;xp,yn)	LMM Auger	3.45 - 5.07	7	100	2	155-65-2-1	+
$^{159}Dy_{66}$	EC	$^{159}Tb_{65}$	144.4(2) d	Ta(p;xp,yn)	Review	0.3 - 9.8	10	150	10	159-66-2-1	
					Review (log scale)	0.3 - 9.8	10	150	10	159-66-2-2	+
					LMM Auger	5.55 - 6.27	3.5	50	2	159-66-2-3	

1	2	3	4	5	6	7	8	9	10	11	12
$^{160}Er_{68}$	EC	$^{160}Ho_{67}$	28.58(9) d	Ta(p;xp,yn)	Review	0.35 - 8.0	3.5	50	2	160-68-2-1	
	EC	$^{160}Dy_{66}$	25.6(3) m		Review (log scale)	0.35 - 8.0	3.5	50	2	160-68-2-2	+
$^{165}Er_{68}$	EC	$^{165}Ho_{67}$	10.34(5) h	Ta(p;xp,yn)	LMX Auger	3.7 - 8.2	7	100	5	165-68-2-1	+
$^{167}Tm_{69}$	EC	$^{167}Er_{68}$	9.25(2) d	Ta(p;xp,yn)	LMX Auger	3.8 - 5.8	7	100	2	167-69-2-1	+
					$L_3M_{1-5}M_{1-5}$ Auger	5.15 - 5.87	7	100	1	167-69-2-2	
$^{169}Yb_{70}$	EC	$^{169}Tm_{69}$	32.02(4) d	Ta(p;xp,yn)	Review	0.31 - 20.2	10	150	10	169-70-2-1	
					Review (log scale)	0.31 - 20.2	10	150	10	169-70-2-2	+
					Coster-Kronig LLX transitions	0.21 -2.15	7	100	2	169-70-2-3	
					MNX Auger + Coster-Kronig transitions	0.21 -2.15	7	100	2	169-70-2-4	
					$L_3M_{1-5}M_{1-5}$ Auger	3.9 - 5.8	7	100	2	169-70-2-5	
					$L_3M_{4,5}M_{4,5}$ Auger	5.3 - 5.77	7	100	1	169-70-2-6	
$^{171}Lu_{71}$	EC, β+	$^{171}Yb_{70}$	8.22(3) d	Ta(p;xp,yn)	Review	0.21 - 10.44	7	100	10	171-71-2-1	
					Review (log scale)	0.21 - 10.44	7	100	10	171-71-2-2	+
					LMX Auger	2.6 - 7.8	7	100	5	171-71-2-3	
					L_{1-3}19.4 ICEs	8.6 - 10.65	3.5	50	2	171-71-2-4	
$^{172}Lu_{71}$	EC, β+	$^{172}Yb_{70}$	6.70(4) d	Ta(p;xp,yn)	Review	0.72 - 18.1	21	300	10	172-71-2-1	
					Review (log scale)	0.72 - 18.1	21	300	10	172-71-2-2	+
					LMX Auger	3.6 - 9.1	21	300	5	172-71-2-3	
					K78.4 ICEs	17.1 -17.6	7	100	2	172-71-2-4	
$^{175}Hf_{72}$	EC	$^{175}Lu_{71}$	70(2) d	$^{174}Hf(n,\gamma)$	Review	1.1 - 22.5	35	500	30	175-72-2-1	
					Review (log scale)	1.1 - 22.5	35	500	30	175-72-2-2	+
					K89.4 ICEs	25.8 - 26.3	14	200	5	175-72-2-3	
$^{225}Ac_{89}$	α	$^{221}Fr_{87}$	10.0(1) d	descendant ^{229}Th $^{229}Th(\alpha)$ $^{225}Ra(\beta-)$	Review (log scale)	0.7 - 26.6	21	300	10	225-89-2-1	+
					$M_{1,2}$10.6 ICEs	5.5 - 9.75	21	300	5	225-89-2-2	
					L_{1-3}26.0, M_{1-3}26.0, L_{4-3}36.6, L_{4-3}38.5 ICEs	10.65 -..- 23.7	21	300	10	225-89-2-3	
$^{241}Pu_{94}$	β-	$^{241}Am_{95}$	14.355(7) y	^{238}U multi n-capture	Review	2.2 - 22.0	65	1005	30	241-94-2-1	
					Review (log scale)	2.2 - 22.0	65	1005	30	241-94-2-2	+

1	2	3	4	5	6	7	8	9	10	11	12
$^{241}Am_{95}$	α	$^{237}Np_{93}$	432.0(2) y	$^{241}Pu(\beta^-)$	Review	2.2 - 24.2	7	100	15	241-95-2-1	
					Review (log scale)	2.2 - 24.2	7	100	15	241-95-2-2	+
					$L_{1,3}$26.3, $M_{1,3}$26.3 ICEs	2.6 - 22.6	21	300	5	241-95-2-3	
					$L_{1,3}$43.4 ICEs	19.08 -22.53	7	100	15	241-95-2-4	

Quantity of nuclei 33

Quantity of spectra 114 33

*) ICEs - Internal Conversion Electrons of correspondent (sub)shell of nuclear transition with pointed energy

Table 2. Reference list with the experimental data resulted from the measured spectra.

Source nucleus	Decay mode	Daughter nucleus	Spectrum Code	Reference Code	Reference
1	2	3	4	5	6
$^{51}Cr_{24}$	EC	$^{51}V_{23}$	51-24-2-1 51-24-2-2		A.Kovalik, M.Rysavy, V.Brabec, O.Dragoun, A.Inoyatov, A.F.Novgorodov, Ts.Vylov, and I.A.Prostakov **Physica Scripta, 37(1988) 871-875** The KLL and KLM Auger electrons of vanadium and chromium from radioactive decay
$^{54}Mn_{25}$	EC	$^{54}Cr_{24}$	54-25-2-1 54-25-2-2		A.Kovalik, M.Rysavy, V.Brabec, O.Dragoun, A.Inoyatov, A.F.Novgorodov, Ts.Vylov, and I.A.Prostakov **Physica Scripta, 37(1988) 871-875** The KLL and KLM Auger electrons of vanadium and chromium from radioactive decay
$^{55}Fe_{26}$	EC	$^{55}Mn_{25}$	55-26-2-1 55-26-2-2 55-26-2-3		A.Kovalik, V.Brabec, V.M.Gorozhankin, J.Novak, O.Dragoun, A.F.Novgorodov, Ts.Vylov **Journal of Electron Spectroscopy and Related Phenomena, 50(1990)89-101** The K-Auger spectrum of manganese from ^{55}Fe decay
$^{57}Co_{27}$	EC	$^{57}Fe_{26}$	57-27-2-1 57-27-2-2 57-27-2-3 57-27-2-4 57-27-2-5 57-27-2-6 57-27-2-7		A.Kovalik, V.M.Gorozhankin, Ts.Vylov, D.V.Filosofov, N.Coursol, E.A.Yakushev, Ch.Briancon, A.Minkova, M.Rysavy, O.Dragoun **Journal of Electron Spectroscopy and Related Phenomena, 95(1998)1-24** The low-energy electron spectrum from the EC-decay of ^{57}Co: 0 eV up to 15 keV A.Kovalik, A.Inoyatov, A.F.Novgorodov, V.Brabec, M.Rysavy, Ts.Vylov, O.Dragoun, and A.Minkova. **J.Phys. B: At. Mol. Phys., 20(1987)3997** K Auger spectrum of iron from the ^{57}Co decay
$^{63}Ni_{28}$	β^-	$^{63}Cu_{29}$	63-28-2-1		
$^{73}As_{33}$	EC	$^{73}Ge_{32}$	73-33-2-1 73-33-2-2 73-33-2-3 73-33-2-4 73-33-2-5 73-33-2-6		A.Kovalik, E.A.Yakushev, D.V.Filosofov, V.M.Gorozhankin, Ts.Vylov **Journal of Electron Spectroscopy and Related Phenomena, (2001)** The first experimental investigation of the KLL Auger spectrum of Ge (Z=32)

1	2	3	4	5	6
$^{83}Rb_{37}$	EC	$^{83}Kr_{36}$	83-37-2-1 83-37-2-2 83-37-2-3 83-37-2-4 83-37-2-5 83-37-2-6 83-37-2-7 83-37-2-8		A.Kovalik, V.M.Gorozhankin, A.F.Novgorodov, A.Minkova, M.A.Mahmoud **Journal of Electron Spectroscopy and Related Phenomena, 58(1992)49-66** The K and LMX Auger spectra of krypton from the ^{83}Rb decay A.Kovalik, V.M.Gorozhankin **J.Phys. G: Nucl. Part. Phys., 19(1993)1921-1927** A conversion-electron investigation of the 9.4 keV M1+E2 transition in ^{83}Kr
$^{103}Pd_{46}$	EC	$^{103}Rh_{45}$	103-46-2-1 103-46-2-2 103-46-2-3		
$^{111}In_{49}$	EC	$^{111}Cd_{48}$	111-49-2-1 111-49-2-2 111-49-2-3 111-49-2-4 111-49-2-5 111-49-2-6 111-49-2-7 111-49-2-8 111-49-2-9		A.Kovalik, E.A.Yakushev, D.V.Filosofov, V.M.Gorozhankin, P.A.Petev, M.A.Mahmoud **Journal of Electron Spectroscopy and Related Phenomena, 105(1999)219-229** Precise measurement of the KLL and KLX Auger spectra of cadmium from the EC-decay of ^{111}In
$^{131}I_{53}$	β^-	$^{131}Xe_{54}$	131-53-2-1 131-53-2-2 131-53-2-3 131-53-2-4		A.Kovalik, V.M.Gorozhankin, A.F.Novgorodov, M.A.Mahmoud, N.Coursol, E.A.Yakushev, V.V.Tsupko-Sitnikov **Journal of Electron Spectroscopy and Related Phenomena, 95(1998)231-254** The electron spectrum from the atomic deexcitation of the $^{131}Xe_{54}$
$^{131}Cs_{55}$	EC	$^{131}Xe_{54}$	131-55-2-1 131-55-2-2 131-55-2-3 131-55-2-4 131-55-2-5 131-55-2-6		A.Kovalik, V.M.Gorozhankin, A.F.Novgorodov, M.A.Mahmoud, N.Coursol, E.A.Yakushev, V.V.Tsupko-Sitnikov **Journal of Electron Spectroscopy and Related Phenomena, 95(1998)231-254** The electron spectrum from the atomic deexcitation of the $^{131}Xe_{54}$

1	2	3	4	5	6
$^{140}Nd_{60}$	EC EC	$^{140}Pr_{59}$ $^{140}Ce_{58}$	140-60-2-1 140-60-2-2 140-60-2-3 140-60-2-4 140-60-2-5		A.Kovalik, E.A.Yakushev, D.V.Filosofov, V.M.Gorozhankin, P.A.Petev, I.Stekl **Journal of Electron Spectroscopy and Related Phenomena, 107(2000)239-252** An experimental investigation of some KLL and L_3MM Auger transitions for Z=58, 59, and 61: the predicted relativistic effects on the KL_1L_2 ($^3P_0$) Auger transition probability proved
$^{145}Sm_{62}$	EC EC	$^{145}Pm_{61}$ $^{145}Nd_{60}$	145-62-2-1 145-62-2-2 145-62-2-3 -		A.Kovalik, E.A.Yakushev, D.V.Filosofov, V.M.Gorozhankin, P.A.Petev, I.Stekl **Journal of Electron Spectroscopy and Related Phenomena, 107(2000)239-252** An experimental investigation of some KLL and L_3MM Auger transitions for Z=58, 59, and 61: the predicted relativistic effects on the KL_1L_2 ($^3P_0$) Auger transition probability proved
$^{146}Eu_{63}$	EC, β^+	$^{146}Sm_{62}$	146-63-2-1		
$^{155}Eu_{63}$	β^-	$^{155}Gd_{64}$	155-63-2-1 155-63-2-2 155-63-2-3 155-63-2-4 155-63-2-5		A.Kovalik, V.M.Gorozhankin, A.F.Novgorodov **Journal of Electron Spectroscopy and Related Phenomena, 60(1992)71-100** The L Auger spectra of $^{155}Gd_{64}$, $^{159}Tb_{65}$, $^{165}Ho_{67}$, and $^{171}Yb_{70}$ from radioactive decay
$^{155}Tb_{65}$	EC	$^{155}Gd_{54}$	155-65-2-1		
$^{159}Dy_{66}$	EC	$^{159}Tb_{65}$	159-66-2-1 159-66-2-2 159-66-2-3 - - -		A.Kovalik, V.M.Gorozhankin, A.F.Novgorodov **Journal of Electron Spectroscopy and Related Phenomena, 60(1992)71-100** The L Auger spectra of $^{155}Gd_{64}$, $^{159}Tb_{65}$, $^{165}Ho_{67}$, and $^{171}Yb_{70}$ from radioactive decay A.Kovalik, A.F.Novgorodov, V.M.Gorozhankin, E.A.Yakushev, M.A.Mahmoud, P.Petev **Journal of Electron Spectroscopy and Related Phenomena, 87(1997)1-7** Effects of relativity on the $KL_1L_2(^3P_0)$ Auger transition rate of $^{159}Tb_{65}$
$^{160}Er_{68}$	EC EC	$^{160}Ho_{67}$ $^{160}Dy_{66}$	160-68-2-1 160-68-2-2 - -		V.M.Gorozhankin, A.Kovalik, V.G.Kalinnikov, Ts.Vylov, K.Ya.Gromov, N.A.Lebedev, A.F.Novgorodov, O.Dragoun, V.Brabec, and S.K.Vasiliev **J.Phys. G: Nucl. Part. Phys., 16(1990)99** Experimental evidence for missing low-energy transition in the ^{160}Er-^{160}Ho decay
$^{165}Er_{68}$	EC	$^{165}Ho_{67}$	165-68-2-1 - -		A.Kovalik, V.M.Gorozhankin, A.F.Novgorodov **Journal of Electron Spectroscopy and Related Phenomena, 60(1992)71-100** The L Auger spectra of $^{155}Gd_{64}$, $^{159}Tb_{65}$, $^{165}Ho_{67}$, and $^{171}Yb_{70}$ from radioactive decay

1	2	3	4	5	6
$^{167}Tm_{69}$	EC	$^{167}Er_{68}$	167-69-2-1 167-69-2-2		
$^{169}Yb_{70}$	EC	$^{169}Tm_{69}$	169-70-2-1 169-70-2-2 169-70-2-3 169-70-2-4 169-70-2-5 169-70-2-6		A.Kovalik, A.Minkova, Ts.Vylov, R.J.Walen, Ch.Briancon **Journal of Electron Spectroscopy and Related Phenomena, 83(1997)181-191** The predicted influence of relativistic effects on the $KL_1L_2(^3P_0)$ Auger transition intensity of thulium proved
$^{171}Lu_{71}$	EC, β^+	$^{171}Yb_{70}$	171-71-2-1 171-71-2-2 171-71-2-3 171-71-2-4		A.Kovalik, V.M.Gorozhankin, A.F.Novgorodov **Journal of Electron Spectroscopy and Related Phenomena, 60(1992)71-100** The L Auger spectra of $^{155}Gd_{64}$, $^{159}Tb_{65}$, $^{165}Ho_{67}$, and $^{171}Yb_{70}$ from radioactive decay
$^{172}Lu_{71}$	EC, β^+	$^{172}Yb_{70}$	172-71-2-1 172-71-2-2 172-71-2-3 172-71-2-4		
$^{175}Hf_{72}$	EC	$^{175}Lu_{71}$	175-72-2-1 175-72-2-2		
$^{225}Ac_{89}$	α	$^{221}Fr_{87}$	225-89-2-1 225-89-2-2 225-89-2-3		
$^{241}Pu_{94}$	β^-	$^{241}Am_{95}$	241-94-2-1 241-94-2-2 - -		O.Dragoun, A.Spalek, M.Rysavy, A.Kovalik, E.A.Yakushev, V.Brabec, A.F.Novgorodov, N.Dragounova, and J.Rizek **J.Phys. G: Nucl. Part. Phys., 25(1999)1839-1858** Search for an admixture of heavy neutrinos in the b-decay of ^{241}Pu
$^{241}Am_{95}$	α	$^{237}Np_{93}$	241-95-2-1 241-95-2-2 241-95-2-3 241-95-2-4		A.Kovalik, E.A.Yakushev, V.M.Gorozhankin, A.F.Novgorodov, and M.Rysavy **J.Phys. G: Nucl. Part. Phys., 24(1998)2247-2252** The low-energy electron spectrum from the a-decay of ^{241}Am

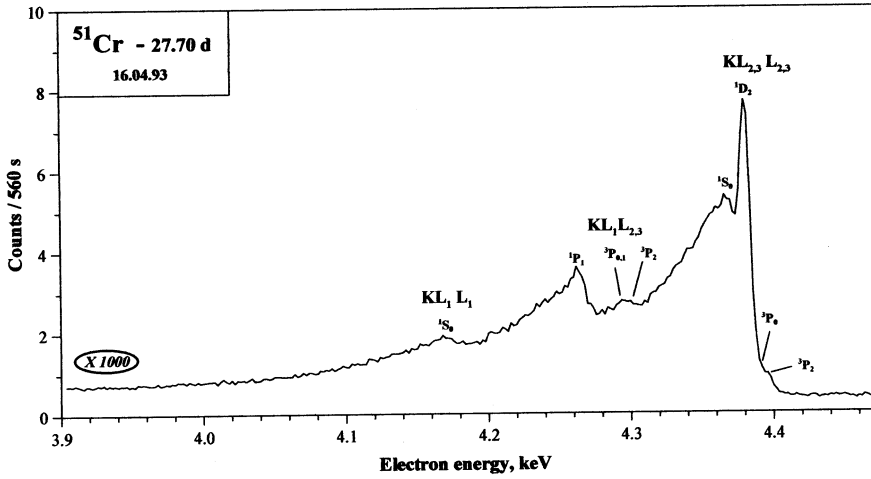
^{51}Cr - 27.70 d
16.04.93
Counts / 560 s
Electron energy, keV
X 1000
KL$_1$ L$_1$
^{1}S$_0$
KL$_1$L$_{2,3}$
^{1}P$_1$
^{3}P$_{0,1}$
^{3}P$_2$
KL$_{2,3}$ L$_{2,3}$
^{1}D$_2$
^{1}S$_0$
^{3}P$_0$
^{3}P$_2$

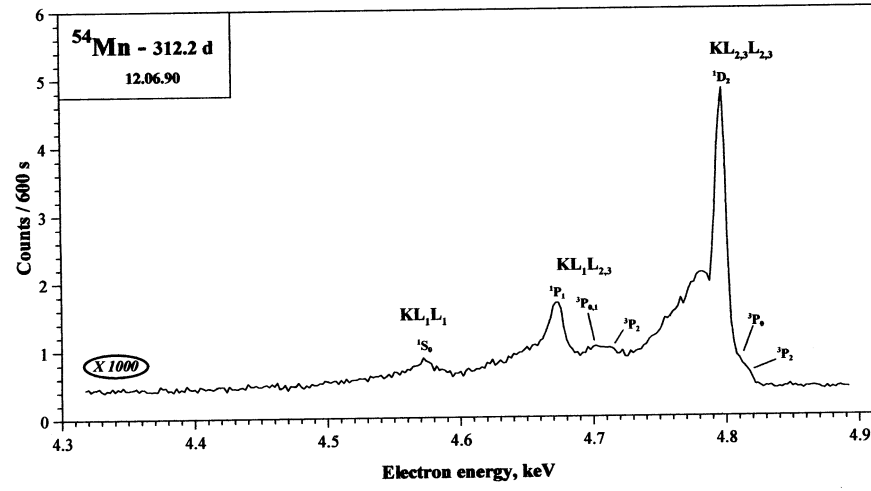
^{54}Mn - 312.2 d
12.06.90
Counts / 600 s
Electron energy, keV
X 1000
KL$_1$L$_1$
^{1}S$_0$
KL$_1$L$_{2,3}$
^{1}P$_1$
^{3}P$_{0,1}$
^{3}P$_2$
KL$_{2,3}$L$_{2,3}$
^{1}D$_2$
^{3}P$_0$
^{3}P$_2$

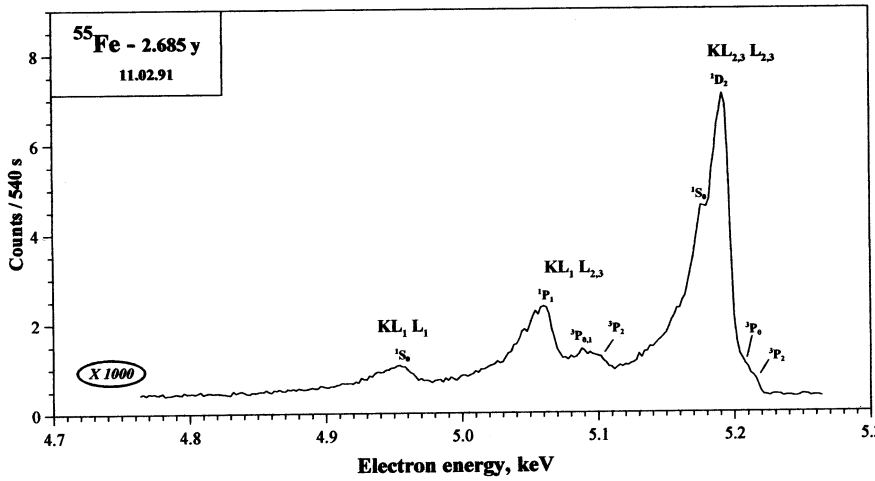
55Fe - 2.685 y
11.02.91
X 1000
Counts / 540 s
Electron energy, keV
KL1 L1
1S0
KL1 L2,3
1P1
3P0,1
3P2
KL2,3 L2,3
1D2
1S0
3P0
3P2

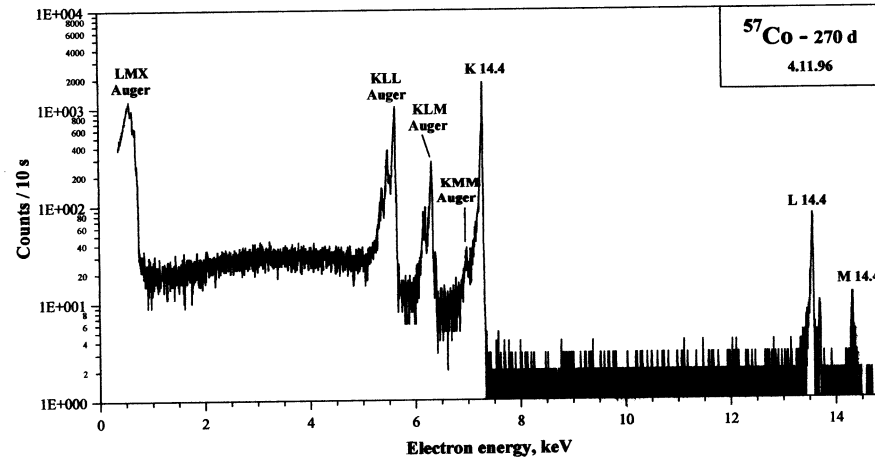
57Co - 270 d
4.11.96
Counts / 10 s
Electron energy, keV
LMX Auger
KLL Auger
KLM Auger
KMM Auger
K 14.4
L 14.4
M 14.4

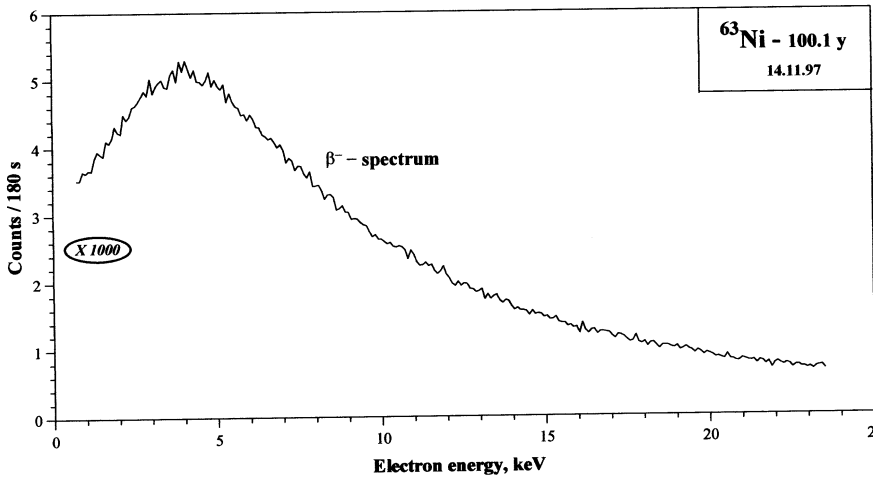
^{63}Ni - 100.1 y
14.11.97
β⁻ – spectrum
X 1000
Counts / 180 s
Electron energy, keV

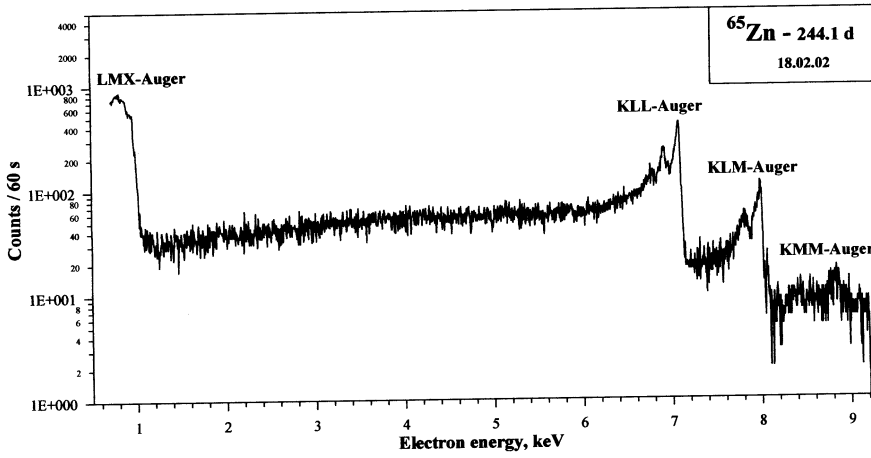
^{65}Zn - 244.1 d
18.02.02
LMX-Auger
KLL-Auger
KLM-Auger
KMM-Auger
Counts / 60 s
Electron energy, keV

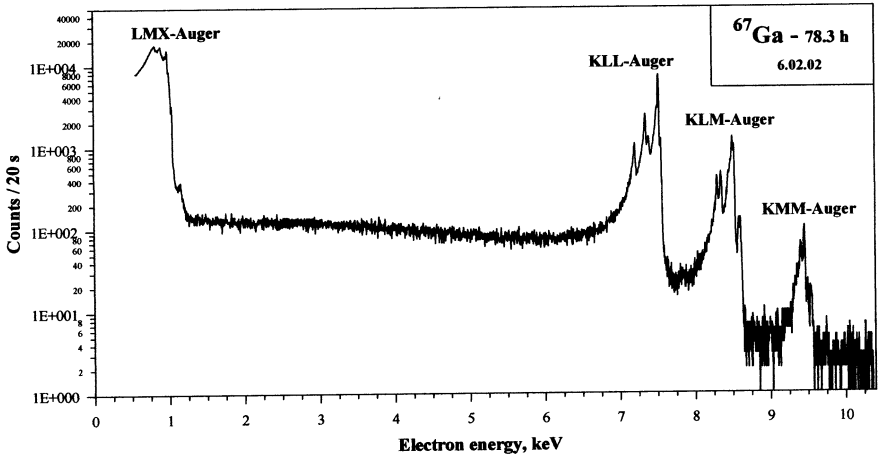
LMX-Auger
KLL-Auger
KLM-Auger
KMM-Auger
67Ga - 78.3 h
6.02.02
Counts / 20 s
Electron energy, keV

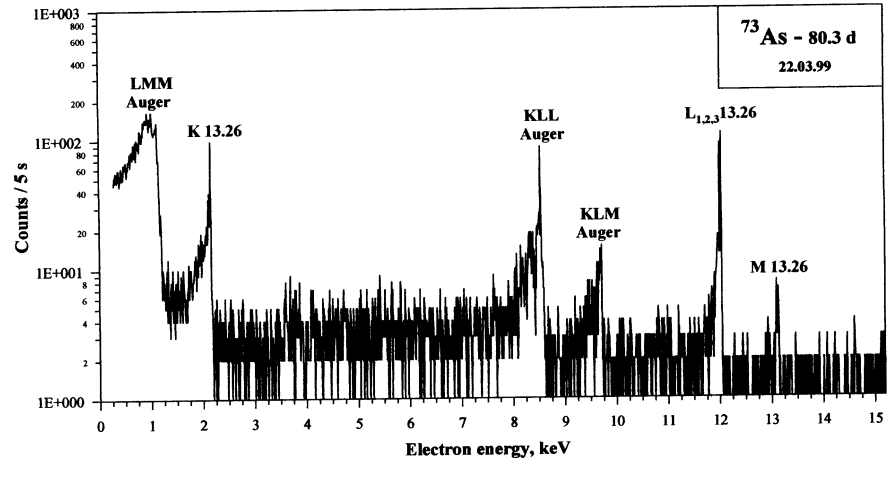
LMM Auger
K 13.26
KLL Auger
KLM Auger
L1,2,3 13.26
M 13.26
73As - 80.3 d
22.03.99
Counts / 5 s
Electron energy, keV

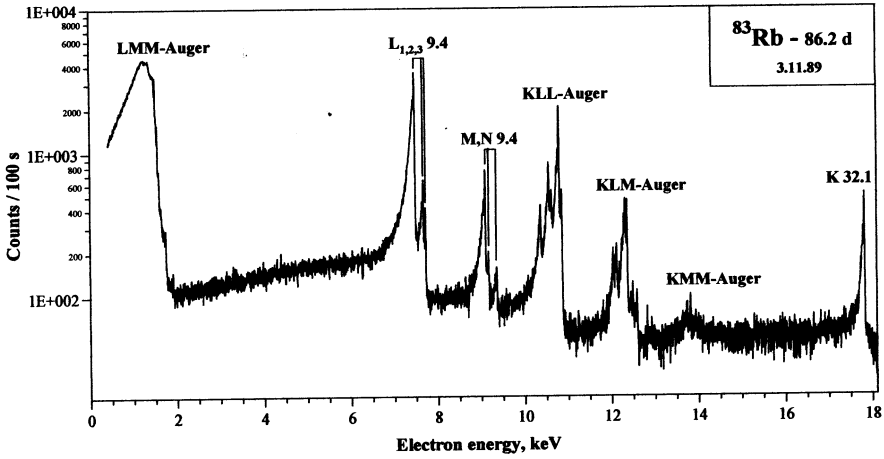
^{83}Rb - 86.2 d
3.11.89
LMM-Auger
$L_{1,2,3}$ 9.4
M,N 9.4
KLL-Auger
KLM-Auger
K 32.1
KMM-Auger
Counts / 100 s
Electron energy, keV

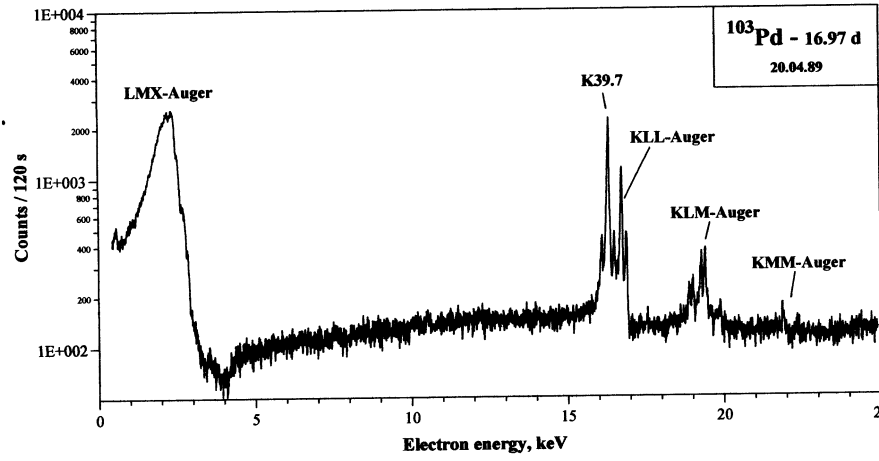
^{103}Pd - 16.97 d
20.04.89
LMX-Auger
K39.7
KLL-Auger
KLM-Auger
KMM-Auger
Counts / 120 s
Electron energy, keV

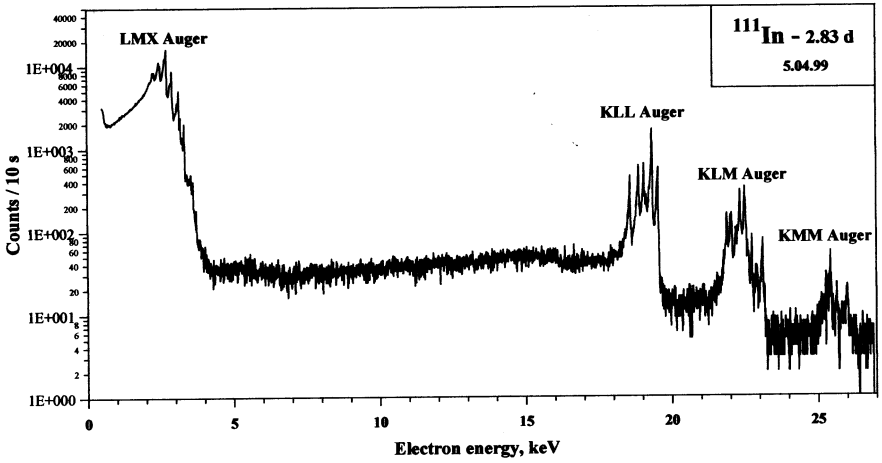
^{111}In - 2.83 d
5.04.99
LMX Auger
KLL Auger
KLM Auger
KMM Auger
Counts / 10 s
Electron energy, keV

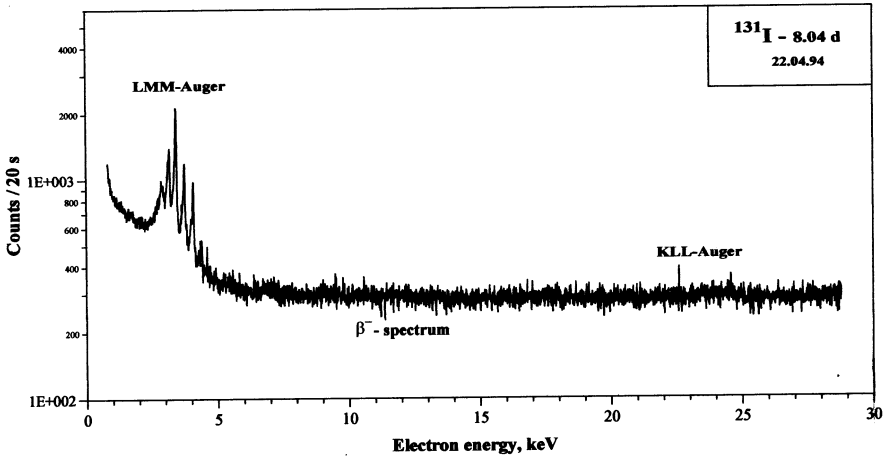
^{131}I - 8.04 d
22.04.94
LMM-Auger
KLL-Auger
β⁻ - spectrum
Counts / 20 s
Electron energy, keV

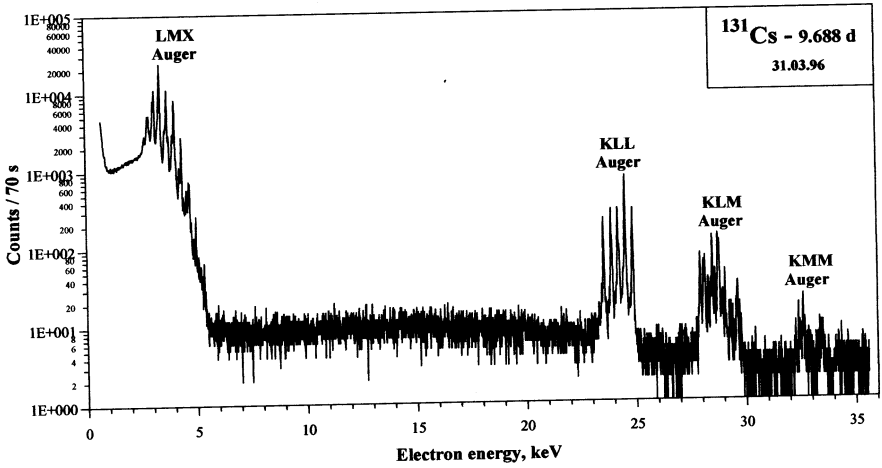
131Cs - 9.688 d
31.03.96
LMX
Auger
KLL
Auger
KLM
Auger
KMM
Auger
Counts / 70 s
Electron energy, keV

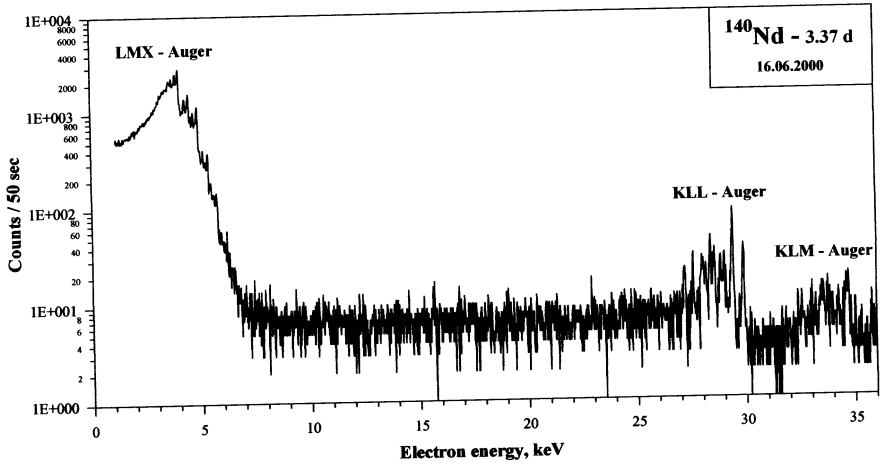
140Nd - 3.37 d
16.06.2000
LMX - Auger
KLL - Auger
KLM - Auger
Counts / 50 sec
Electron energy, keV

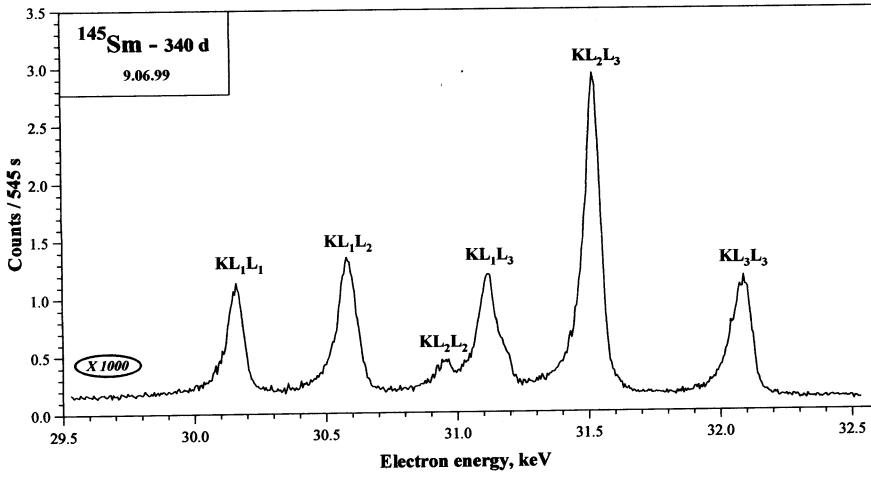
145Sm - 340 d
9.06.99
KL1L1
KL1L2
KL2L2
KL1L3
KL2L3
KL3L3
X 1000
Counts / 545 s
Electron energy, keV

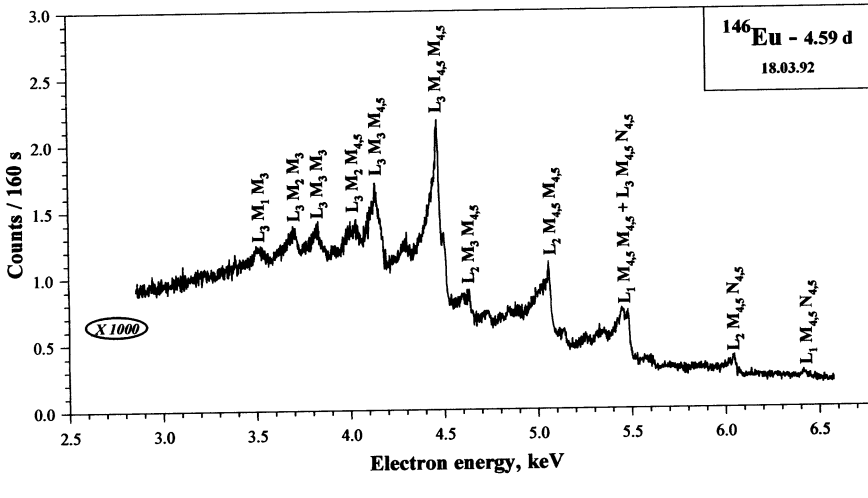
146Eu - 4.59 d
18.03.92
L3 M1 M3
L3 M2 M3
L3 M3 M3
L3 M2 M4,5
L3 M3 M4,5
L3 M4,5 M4,5
L2 M3 M4,5
L2 M4,5 M4,5
L1 M4,5 M4,5 + L3 M4,5 N4,5
L2 M4,5 N4,5
L1 M4,5 N4,5
X 1000
Counts / 160 s
Electron energy, keV

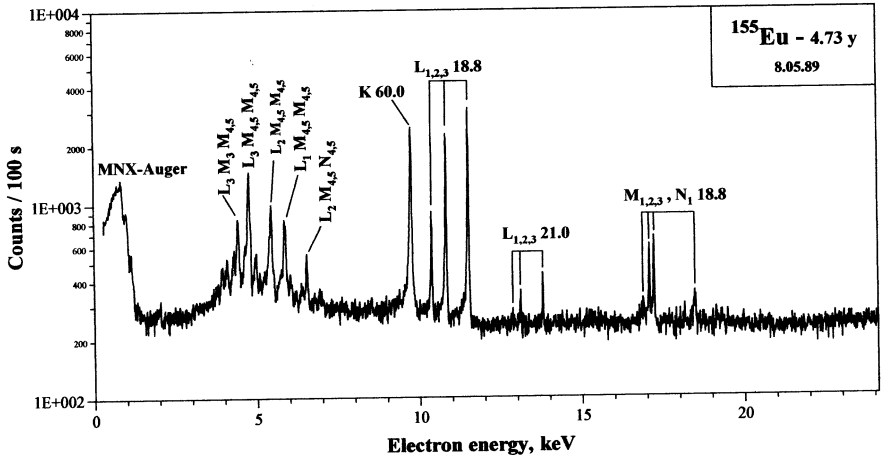
155Eu - 4.73 y
8.05.89
Counts / 100 s
Electron energy, keV
MNX-Auger
L3 M3 M4,5
L3 M4,5 M4,5
L2 M4,5 M4,5
L1 M4,5 M4,5
L2 M4,5 N4,5
K 60.0
L1,2,3 18.8
L1,2,3 21.0
M1,2,3 , N1 18.8

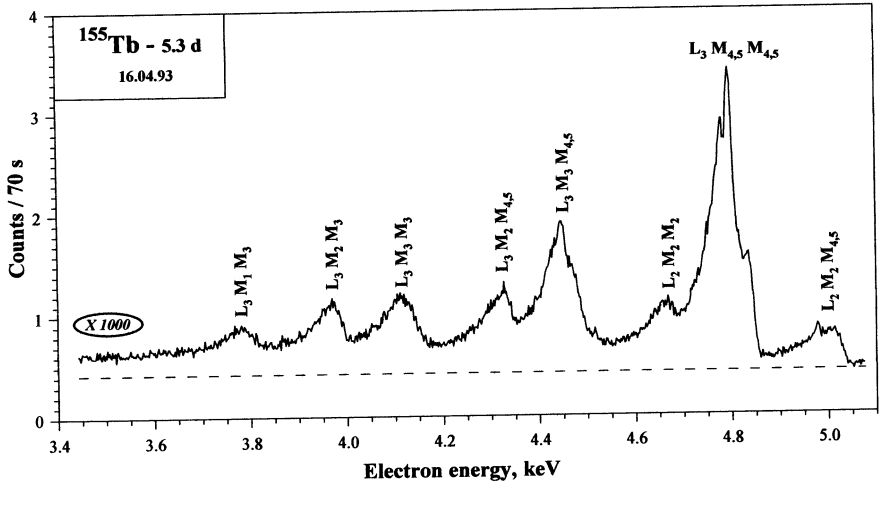
155Tb - 5.3 d
16.04.93
Counts / 70 s
Electron energy, keV
X 1000
L3 M1 M3
L3 M2 M3
L3 M3 M3
L3 M2 M4,5
L3 M3 M4,5
L2 M2 M2
L3 M4,5 M4,5
L2 M2 M4,5

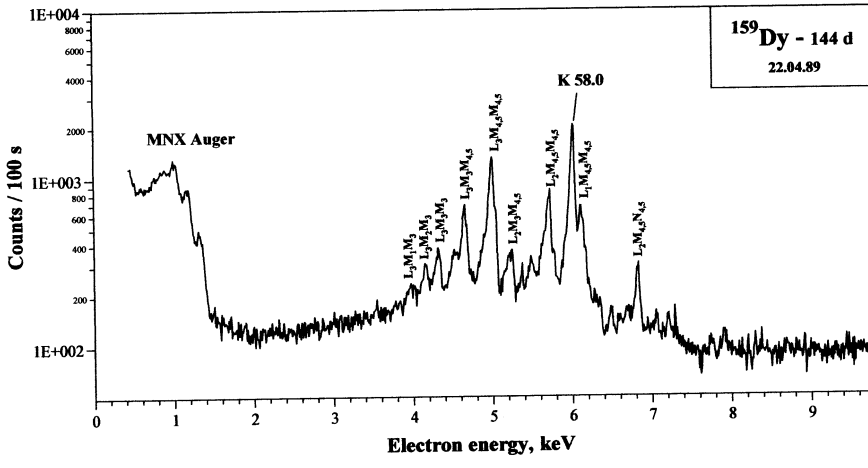
159Dy - 144 d
22.04.89
K 58.0
MNX Auger
Counts / 100 s
Electron energy, keV

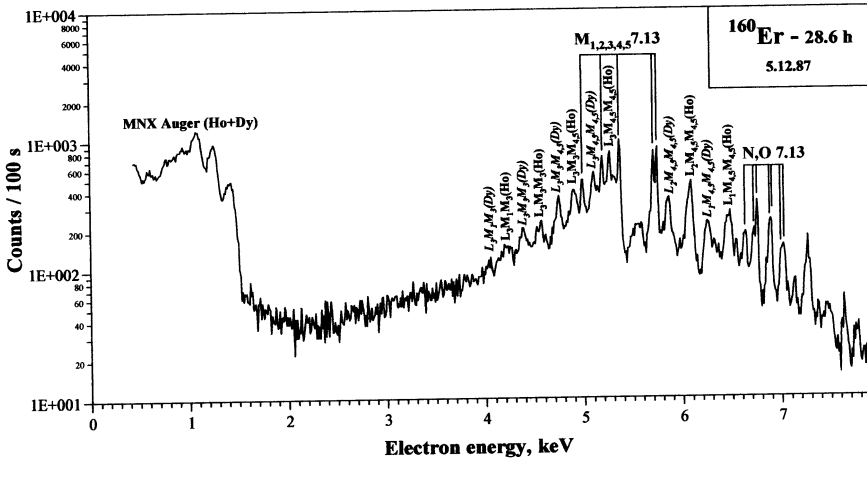
160Er - 28.6 h
5.12.87
M1,2,3,4,5 7.13
MNX Auger (Ho+Dy)
N,O 7.13
Counts / 100 s
Electron energy, keV

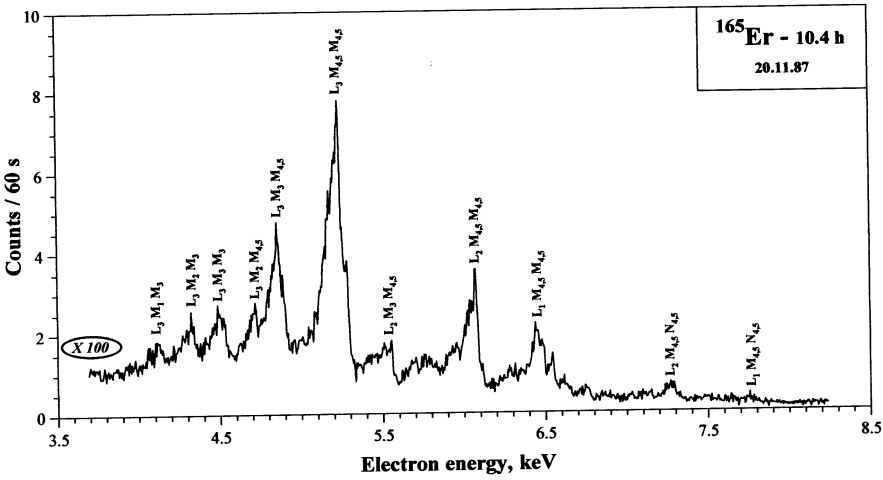
^{165}Er - 10.4 h
20.11.87
Counts / 60 s
Electron energy, keV
X 100
$L_3 M_1 M_3$
$L_3 M_2 M_3$
$L_3 M_3 M_3$
$L_3 M_2 M_{4,5}$
$L_3 M_3 M_{4,5}$
$L_3 M_{4,5} M_{4,5}$
$L_1 M_3 M_{4,5}$
$L_2 M_{4,5} M_{4,5}$
$L_1 M_{4,5} M_{4,5}$
$L_2 M_{4,5} N_{4,5}$
$L_1 M_{4,5} N_{4,5}$

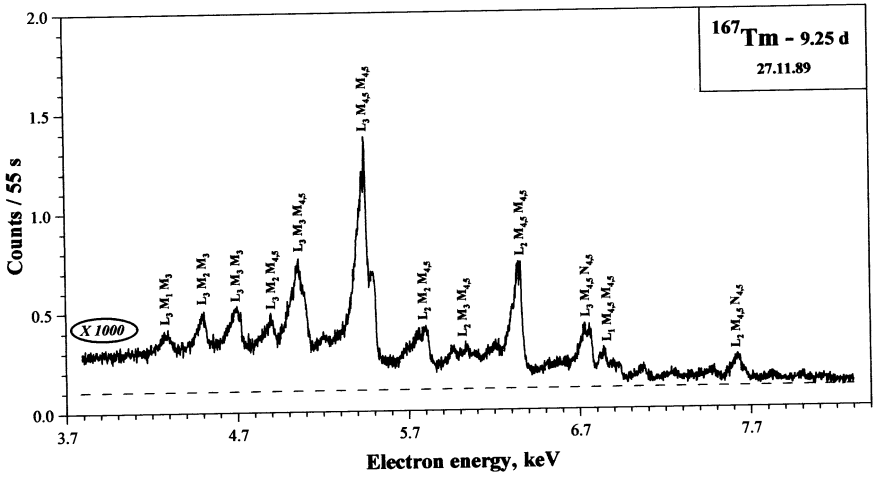
^{167}Tm - 9.25 d
27.11.89
Counts / 55 s
Electron energy, keV
X 1000
$L_3 M_1 M_3$
$L_3 M_2 M_3$
$L_3 M_3 M_3$
$L_3 M_2 M_{4,5}$
$L_3 M_3 M_{4,5}$
$L_3 M_{4,5} M_{4,5}$
$L_2 M_1 M_{4,5}$
$L_2 M_3 M_{4,5}$
$L_2 M_{4,5} M_{4,5}$
$L_3 M_{4,5} N_{4,5}$
$L_1 M_{4,5} M_{4,5}$
$L_2 M_{4,5} N_{4,5}$

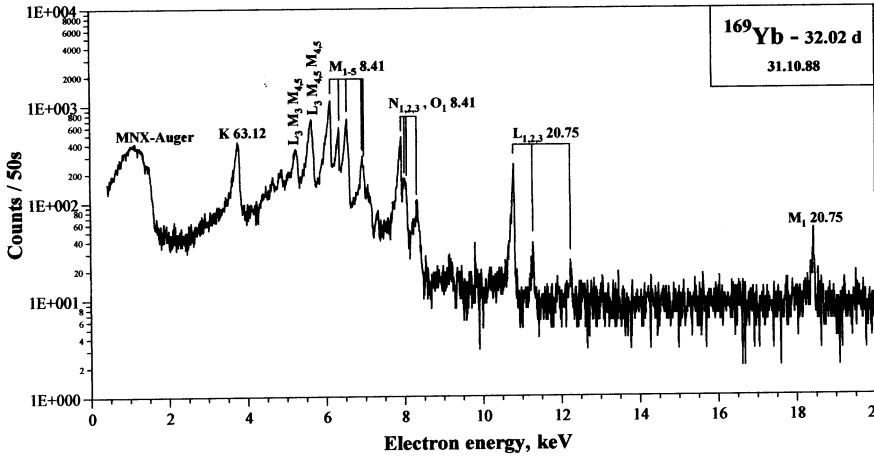
169Yb - 32.02 d
31.10.88
MNX-Auger
K 63.12
L3 M4,5 M4,5
L3 M4,5 M4,5
M1-5 8.41
N1,2,3 , O1 8.41
L1,2,3 20.75
M1 20.75
Counts / 50s
Electron energy, keV

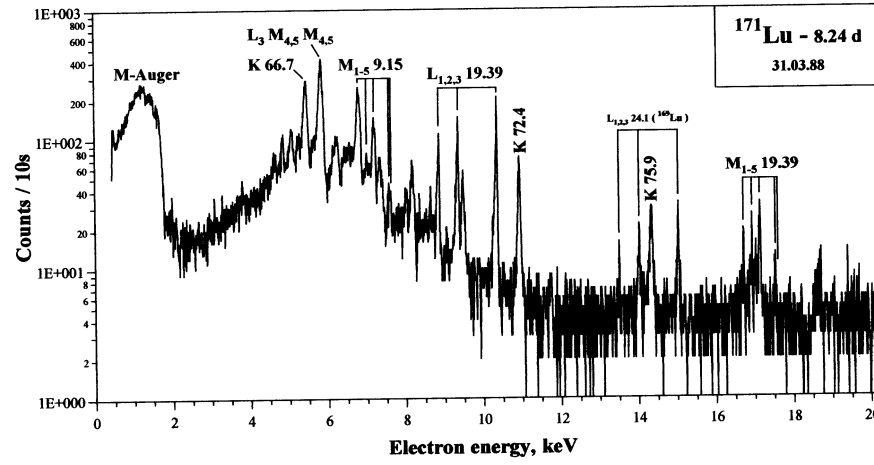
171Lu - 8.24 d
31.03.88
M-Auger
L3 M4,5 M4,5
K 66.7
M1-5 9.15
L1,2,3 19.39
K 72.4
L1,2,3 24.1 (169Lu)
K 75.9
M1-5 19.39
Counts / 10s
Electron energy, keV

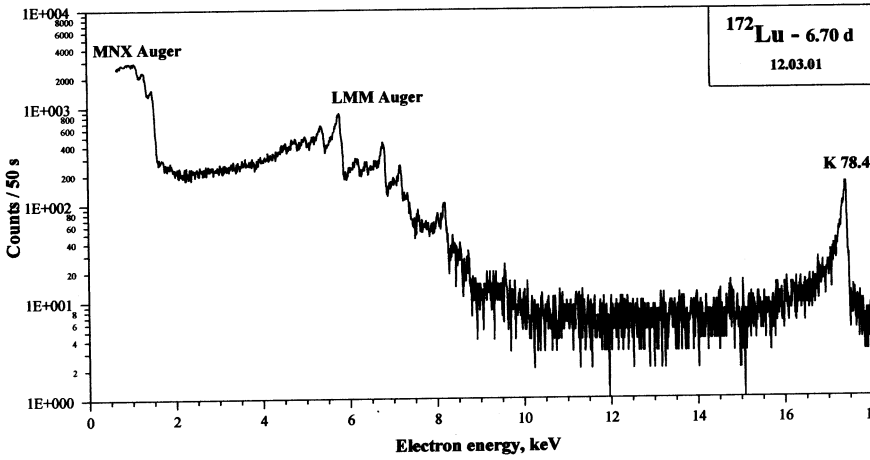
^{172}Lu - 6.70 d
12.03.01
MNX Auger
LMM Auger
K 78.4
Counts / 50 s
Electron energy, keV

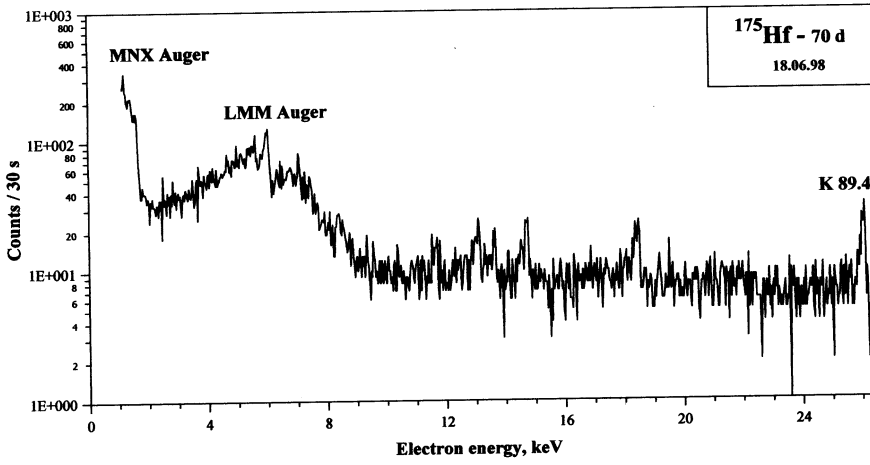
^{175}Hf - 70 d
18.06.98
MNX Auger
LMM Auger
K 89.4
Counts / 30 s
Electron energy, keV

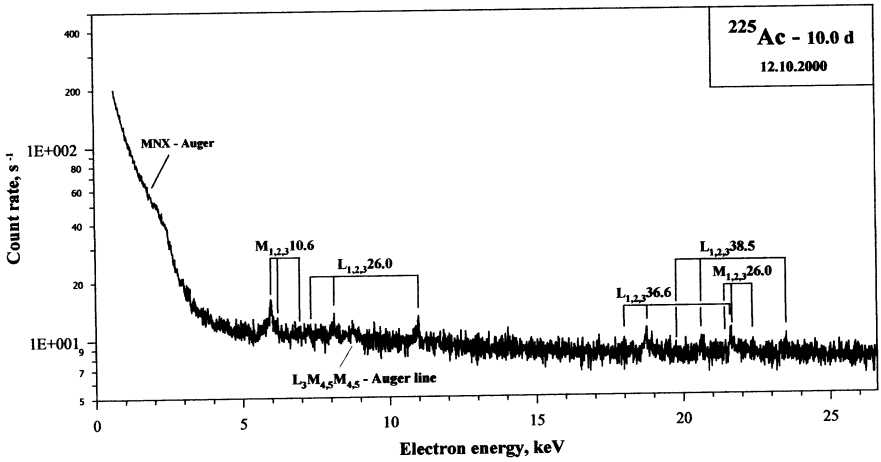
225Ac - 10.0 d
12.10.2000
MNX - Auger
M1,2,310.6
L1,2,326.0
L1,2,338.5
M1,2,326.0
L1,2,336.6
L3M4,5M4,5 - Auger line
Count rate, s-1
Electron energy, keV

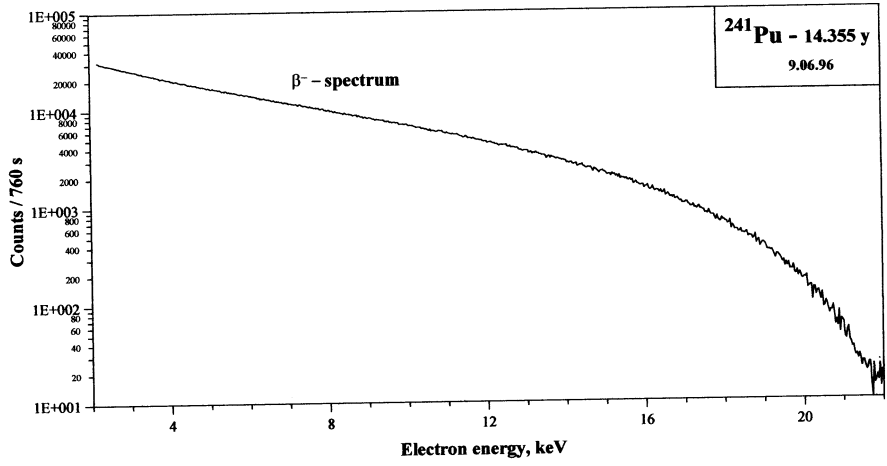
241Pu - 14.355 y
9.06.96
β− – spectrum
Counts / 760 s
Electron energy, keV

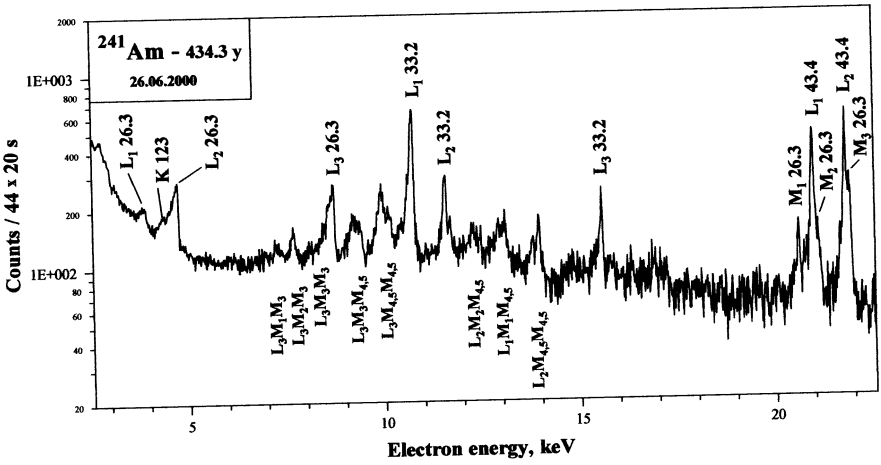
241Am - 434.3 y
26.06.2000
Counts / 44 x 20 s
Electron energy, keV
L1 26.3
K 123
L2 26.3
L3 26.3
L1 33.2
L2 33.2
L3 33.2
M1 26.3
L1 43.4
M2 26.3
L2 43.4
M3 26.3
L3M1M3
L3M2M3
L3M3M3
L3M3M4,5
L3M4,5M4,5
L2M2M4,5
L1M1M4,5
L2M4,5M4,5

References

1. Abdurazakov A.A., et al. Atlas of internal conversion electron spectrum of neutron deficient radionucleous in A=131-172 region. Tashkent, "Uzbekiston", 1991. (in russian)
2. Siegbahn K. In: Alpha-, beta-, and gamma-spectroscopy, ed. K Siegbahn, "Atomizdat", Moscow, 1969, p.96-213. (in russian)
3. Mladenovich M.S. Development of magnetic beta-ray spectroscopy. – "Springer", Berlin and New-York, 1976.
4. Siegbahn K., Nordling K., et al. Electron spectroscopy. "Mir", Moscow, 1971. (in russian)
5. Sevier K.D. Low energy electron spectrometry. – "Wileg-Interscience", New-York, 1972.
6. Carlson T. Photo and Auger electron spectroscopy. "Mashinostroenie", Leningrad, 1981. (in russian)
7. Parker B., Slatis G. In: Alpha-, beta-, and gamma-spectroscopy, ed. K Siegbahn, "Atomizdat", Moscow, 1969, p.380-405. (in russian)
8. Beischer D.E. – J.Phys. Chem., v.57, 1953, p. 134.
   Beisher D.E. Monomolecular layers. Moscow, "Foreign literature", 1956.
9. Briancon Ch., Legrand B. et al. - Nucl. Instrum. and Meth., A221, 1984, p. 547.
10. Legrand B. – Comm. of the Joint Institute for Nuclear Research, E13-83-326, Dubna, 1983.
11. Kovalik A., Inoyatov A. et al. – J. Phys., B,: At. Mol. Phys., v.20, 1987, p. 3997.
12. Was B., Kovalik A. et al. – Nucl. Instr. and Meth., A332, 1993, p. 334.
    Was B., Novgorodov A.F., et al. Communication of JINR P6-92-397, Dubna, 1992.
13. Dobrilovič L., Simovič M. - Nucl. Instr. and Meth., v.112, 1973, p. 359.
14. Simovič M., Dobrilovič L., - J. Radioanal. Chem., v. 44, 1978, p. 345.
15. Dobrilovič L. et al. – Applied Radiat. Isotopes, v. 39, 1988, p. 999.
16. Borchert G.L. – Naturforsh Z., A31, 1976, p. 387.
17. Borchert G.L., Scheck W. Et al. – Naturforsh Z., A30, 1975, p. 274.
18. Lederer C.M., Shirley V.S. Table of Isotopes. 7-th ed. – "Wiley", New-York, 1978, Appendix 3.
19. Kovalik A., Gorozhankin V.M. et al. – J. Phys. G: Nucl. Part. Phys., v. 19, 1993, p.1921.
20. Kovalik A., Yakushev E.A., et al. Proc. of 51 Russian Conference on Nuclear Spectroscopy and Atomic Nuclear Structure, Sarov, 2001, p.239. (in russian).
21. Szajman J., Leckey R.C. – J. Electron Spectrosc. Relat. Phenom. v. 23, 1981, p. 83.
22. Seah M.P., Dench W.A. – SIA Surt. Interface Annal., v.1, 1979, p.1.
23. Špalek A., Dragoun O. - J. Phys. G: Nucl. Part. Phys., v. 19, 1993, p.2071.
24. Baro J., Sempau J. et al. - Nucl. Instrum. and Meth., B100, 1995, p. 31.
25. Ryšavý M., Fišer M. – Comput. Phys. Commun., v. 29, 1983, p. 171.
26. Kovalik A., Gorozhankin V.M. et al. – J. Electron Spectrosc. Relat. Phenom. v. 58, 1992, p. 49.
27. Špalek A., Dragoun O. – Czech. J. Phys., v. 24, 1974, p. 161.
28. James F. – In: Proc. 1972 CERN Computing and Data Processing School, 10 – 24 September 1972, Pertisan, Austria (CERN 72-21).
29. Vylov Tz. Comm. of the Joint Institute for Nuclear Research, E6-2001-35, Dubna, 2001.

Received on February 19, 2003.

Вылов Ц. и др. E6-2003-31
Атлас низкоэнергетических спектров электронов радионуклидов (LEES)

Более 100 аппаратурных спектров низкоэнергетических электронов радионуклидов в области $Z=24-95$ собраны в представленном атласе LEES. Эти спектры являются результатом систематических исследований оже- и конверсионных электронов, проводившихся с помощью электростатического спектрометра ESA-50 на протяжении последних 20 лет.

Работа выполнена в Лаборатории ядерных проблем им. В. П. Джелепова, ОИЯИ, Дубна, в CSNSM (IN2P3-CNRS), Орсэ, Франция, и в BNM-LNHB (LIST/DIMRI), CEA, Сакле, Франция.

Сообщение Объединенного института ядерных исследований. Дубна, 2003

Vylov Tz. et al. E6-2003-31
Catalogue of Radionuclide Low-Energy Electron Spectra (LEES)

More than 100 of apparatus low-energy electron spectra from radionuclides with $Z=24-95$ are collected in the presented LEES Catalogue. These spectra have been recorded in systematical investigations of Auger and internal conversion electrons with the ESA-50 electrostatic spectrometer during past 20 years.

The investigation has been performed at the Dzhelepov Laboratory of Nuclear Problems, JINR, Dubna, at the CSNSM (IN2P3-CNRS), Orsay, France and at the BNM-LNHB (LIST/DIMRI), CEA, Saclay, France.

Communication of the Joint Institute for Nuclear Research. Dubna, 2003

Макет *Т. Е. Попеко*

Подписано в печать 11.03.2003.
Формат 60 × 90/16. Бумага офсетная. Печать офсетная.
Усл. печ. л. 2,25. Уч.-изд. л. 4,23. Тираж 300 экз. Заказ № 53804.

Издательский отдел Объединенного института ядерных исследований
141980, г. Дубна, Московская обл., ул. Жолио-Кюри, 6.
E-mail: publish@pds.jinr.ru
www.jinr.ru/publish/